ELSEVIER

Journal of Crystal Growth 203 (1999) 156–162

JOURNAL OF CRYSTAL GROWTH

Ni^{2+} distribution in $BaLiF_3$ crystals prepared by the zone-melting technique

A.M.E. Santo[1], S.P. Morato, S.L. Baldochi*

Instituto de Pesquisas Energéticas e Nucleares, IPEN-CNEN/SP, Caixa Postal 11049, São Paulo, SP 05422-970, Brazil

Received 27 October 1998; accepted 26 January 1999
Communicated by D.T.J. Hurle

Abstract

$BaLiF_3 : Ni^{2+}$ was synthesized under HF atmosphere with 1, 3 and 5 mol% of nickel concentration in the melt. Ni^0 formation was observed in synthesized ingots even for processes under HF flow. Thermal analysis measurements showed the simultaneous occurrence of oxidation and reduction of nickel during the melt process. The distribution coefficient of Ni^{2+} in the $BaLiF_3$ matrix was evaluated as 0.1 in the zone-melting experiments.

PACS: 81.10.Fq; 81.70.Pg

Keywords: Zone melting; Barium lithium fluoride; Thermal analysis

1. Introduction

Transition-metal ions in $BaLiF_3$ crystals give rise to broad-band emissions which are potentially useful as vibronic laser material [1]. Spectroscopic studies of $BaLiF_3 : Ni^{2+}$ (BLF : Ni) showed an infrared emission band centered at 1.5 μm with an emission cross-section of 3×10^{-21} cm^2 [2]. Considering practical laser development, this small cross section requires crystals with high dopant concentrations. However, a concentration quenching effect was also observed in $BaLiF_3 : Ni^{2+}$. This effect reduces the luminescence decay time and consequently limits the maximum ideal concentration to 1 mol% [3]. This means that to obtain laser emission in this matrix it is necessary to prepare long samples, above 2 cm length, with good optical quality.

The preparation of fluoride crystals with high optical quality for laser applications depends not only on the growth procedures but also on the purity of the raw material used in growth. Samples with these characteristics were obtained by the Czochralski method under a reactive atmosphere of CF_4 [4] and frequently lead to the formation of a thin metallic film on the melt surface. Nickel fluoride, like other transition metal fluorides,

* Corresponding author. Fax: + 55-11-816-9315.
E-mail address: baldochi@net.ipen.br (S.L. Baldochi)
[1] EMGEPRON/CTMSP – Brazilian Navy Technological Center in São Paulo.

0022-0248/99/$ – see front matter
PII: S0022-0248(99)00077-9

undergoes reduction and/or oxidation easily, resulting in the formation of this film which disturbs the dopant distribution in the Czochralski-grown crystals. Consequently, it is very important to search for a method to directly incorporate the dopant in the matrix prior to crystal growth. The incorporation of Ni^{2+} in BLF crystals for optical applications was studied using the zone-melting technique under reactive atmosphere. In the present work, the stoichiometric variations during the material synthesis, the influence of the dopant in the melting process and the distribution of Ni^{2+} in $BaLiF_3$ crystals were studied.

2. Experimental procedure

The starting materials were prepared by standard hydrofluorination methods [5]. BaF_2 was synthesized from $BaCO_3$ (Johnson Matthey 99.997%), LiF (Aldrich 99.99%) was pre-purified by zone melting and NiF_2 (Aldrich 99 + %) was used as dopant. The raw materials were weighed and mixed in a nonstoichiometric composition, according to the BaF_2–LiF phase diagram [6], with nominal nickel concentrations of 1, 3 and 5 mol%. The synthesis experiments were always preceded by a thermal treatment to eliminate water contamination. The melting of the material was performed under HF atmosphere.

Zone-melting experiments were carried out in vitreous-carbon crucibles inserted in a platinum tubular reactor under HF flow. The total length of the ingots (L) is about 290 mm and the length of the liquid zone (l) is 26 mm. Because of the incongruent melting of BLF, the zone-melting experiments were performed in only one run. The experimental angular correction used to compensate for the difference between the density in the solid and liquid phases was not enough to keep the traversal area of the refined ingots constant. However, the ratio between the mass of the solidified material and the total mass of the ingot was used to calculate the experimental error in the dopant concentration measurement. The incorporation and distribution of the dopant in the prepared ingots were evaluated by neutron activation analysis.

The purity level, the melting behavior and transition temperatures, and variation of stoichiometry were studied by thermal analysis: thermogravimetry (TG) and differential thermal analysis (DTA). The thermal analysis experiments were accomplished in a simultaneous TG/DTA system of TA Instruments, model SDT 2960.

3. Results and discussion

3.1. Synthesis of $BaLiF_3 : Ni^{2+}$

The values of nominal and measured nickel concentrations after synthesis are shown in Table 1. The synthesized material shows approximately 20% reduction in the Ni^{2+}-measured concentration compared to the nominal concentration. This difference can be explained by considering the chemical properties of NiF_2. When nickel fluoride is heated up to high temperatures in the presence of water it can be easily reduced to Ni^0, according to the reaction

$$NiF_2 + H_2O \leftrightarrow Ni^0 + \tfrac{1}{2}O_2 + 2HF. \quad (1)$$

This effect can be observed during the growth of these crystals by the Czochralski method. Even the presence of traces of water in the system induces the reduction of the NiF_2 resulting in a metallic scum on the melt surface. This phenomenon disturbs the growth conditions and also decreases the Ni^{2+} concentration in the melt.

Table 1
Ni^{2+} concentration in $BaLiF_3 : Ni^{2+}$ with nominal concentrations of 1, 3 and 5 mol%

Nominal concentration	1 mol% NiF_2	3 mol% NiF_2	5 mol% NiF_2
Measured Ni^{2+} concentration – C_0 (mol%)	0.810 ± 0.004	2.50 ± 0.03	4.08 ± 0.06

In the synthesis of BLF : Ni under reactive atmosphere (HF), the formation of small metallic spots on the surface of the ingots with nominal concentrations of 3 and 5 mol% Ni^{2+} was also observed. Only in 1 mol%-doped ingots this effect was not observed. It is supposed that the use of a reactive atmosphere during the melting and/or thermal treatment of the material minimizes the effect of reaction (1). Actually, HF reacts with Ni^0 at 225°C and consequently the reaction is shifted to the right side. As the reaction rate is low, the reduction of the NiF_2 is not completely achieved during the process of synthesis resulting in the presence of Ni^0 in the ingots with higher concentrations.

Fig. 1 shows the thermal behavior of commercial NiF_2 obtained by TG. In the TG curve two events of mass-loss can be observed. Step I corresponds to a relative mass-loss of 2.2% of the raw material. This mass-loss is probably related to the evaporation of water adsorbed by the material during the storage period. The dehydration process starts at the onset temperature of about 106°C. The water is not eliminated immediately and there are still some molecules of water strongly bounded, which are continuously evaporated from the raw material at higher temperatures. Platform II corresponds to the material partially dehydrated. A second event is observed at about 400°C and shows a mass-loss of 23%. It is expected that this effect is related to the partial reduction of NiF_2 to Ni^0 due to the presence of water in the system. The efficiency of the reduction reaction is 60.5% and therefore the material at the platform III consists of a mixture of NiF_2 and Ni^0.

The thermal behavior of synthesized BLF doped with Ni^{2+} has been studied to determine if this effect is also observable after dopant incorporation in the host. The TG/DTA curves of the sample doped with 1 mol% Ni^{2+} were obtained using two different atmospheres: (a) helium flow, using a cooper wire trap to remove O^{2-} and a molecular sieve trap to remove small amounts of water present in the gas, and (b) air flow, using a commercial filter in order to remove dust and oil eventually present in the air compression system. TG and DTA curves are shown in Figs. 2 and 3, respectively. DTA curves of Fig. 2 shows two endothermic peaks: the first corresponds to the melting temperature of eutectic due to the excess of LiF in the starting composition and to the addition of the dopant. The second peak corresponds to the melting temperature of the BLF : Ni phase and it is represented by a well-defined narrow peak. Mass loss due to the evaporation of one of the components could be observed from the TG curve just after the melting point. Comparing these curves with the curves of Fig. 3 it is clearly observed that, under air flow, the endothermic melting point peak of BLF : Ni is broadened in its base and TG curve presents a significant mass gain. This effect is related to the oxidation of the Ni^{2+}, which occurs

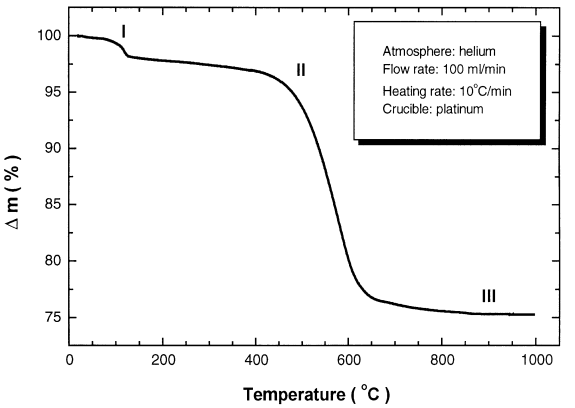

Fig. 1. TG curve of commercial NiF_2 used in the synthesis of $BaLiF_3 : Ni^{2+}$.

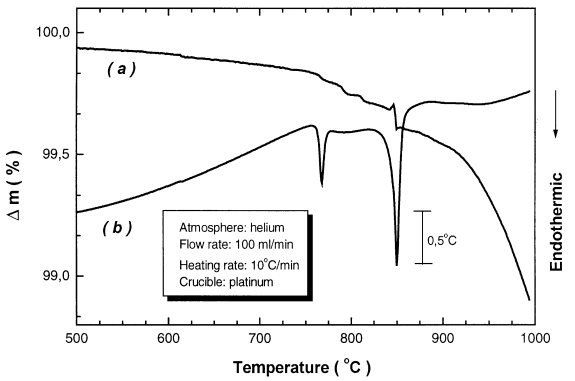

Fig. 2. Thermal analysis curves of $BaLiF_3 : Ni^{2+}$ synthesized with 1 mol% of nickel under He flow: (a) TG curve and (b) DTA curve.

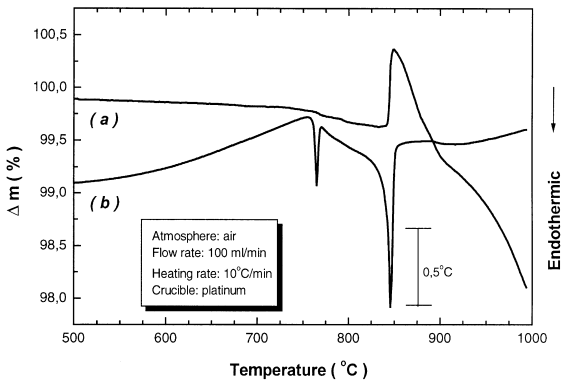

Fig. 3. Thermal analysis curves of $BaLiF_3 : Ni^{2+}$ synthesized with 1 mol% of nickel under filtered air flow: (a) TG curve and (b) DTA curve.

during the melting of the material. This is not clearly visible in the DTA curve due to the simultaneous events of melting and oxidation. These results indicate that besides the problem of the reduction, it is also possible to predict some oxidation of the nickel incorporated in the $BaLiF_3$. These effects occur due to the presence of O_2 and small amounts of water in the air flow, following the reactions:

$$2Ni^{2+} + O_2 \rightarrow 2NiO$$

or

$$Ni^{2+} + 2H_2O \Rightarrow NiO_2 + 4H^+ + 2e. \quad (2)$$

The synthesis experiments were carried out in graphite crucibles under a mixed flux of HF and argon. A slight mass loss of the crucibles was observed after the process. This is an evidence of the presence of impurities in the gas flow. Even traces of water or O^{2-} present in the argon can induce the oxidation reaction in the Ni^{2+} ions.

It is interesting to mention that no variation was observed concerning melting temperature of the different doped materials.

3.2. Zone melting of $BaLiF_3 : Ni^{2+}$

The zone-melting process of an incongruently melting compound results in the separation of the ingot into different regions. A typical zone-refined ingot of pure $BaLiF_3$ presents three regions: the initial part which is opaque and brittle; the central region composed of stoichiometric phase BLF which is bright and transparent; and the final part composed of the eutectic phase which is white opaque and hard. When the starting stoichiometry is 44% BaF_2 : 56% LiF one obtains after zone melting approximately 76% of the total volume of the ingot as the BLF stoichiometric phase [7]. Doped BLF : Ni ingots present similar results, except for the facts that the ingots appear green in color and the volumetric fraction of the stoichiometric phase BLF decreases with increasing dopant level: 63.5 vol% for 1 mol%, 55.1 vol% for 3 mol% and 52.9 vol% for the 5 mol%-doped ingots. This reduction of the available BLF : Ni phase volume with the increase in the nominal concentration of Ni^{2+} is a direct effect of the incongruent melting of the BLF compound.

Using extended X-ray absorption fine-structure spectroscopy (EXAFS), Chadwick et al. [8] have shown that the Ni^{2+} dopant in $BaLiF_3$ predominantly substitutes on the Li^+ site of the host lattice. The first assumption is that the Ni^{2+} ions prefer the Ba^{2+} sites in the $BaLiF_3$ crystal because this operation does not require the formation of charge-compensation effects. However, the effects of ionic radii and the crystal chemistry of the dopant must be also taken into account. Ni^{2+} has a radius of 0.69 Å which is much closer to the radius of Li^+ (0.90 Å) than that of Ba^{2+} (1.49 Å). Furthermore, in other

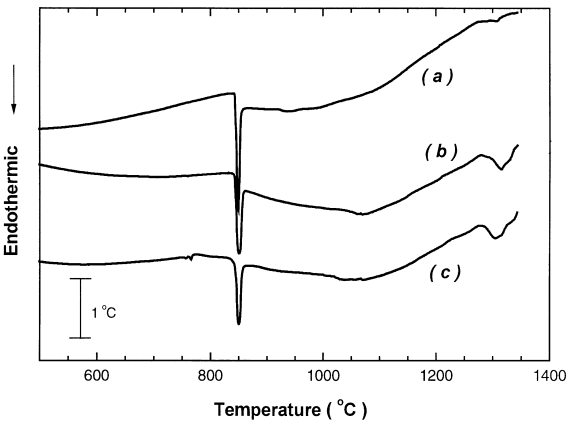

Fig. 4. Heating DTA curves from doped ingots prepared with nominal concentrations of: (a) 1, (b) 3 and (c) 5 mol% of nickel.

Table 2
Ni^{2+} distribution coefficient (k) in the zone-refined $BaLiF_3 : Ni^{2+}$ ingots (L: total ingot length. L^*: stoichiometric region length)

Nominal concentration (mol%)	Neutron activation analysis		X-ray fluorescence analysis	
	L^*	L	L^*	L
1	0.281 ± 0.042	0.207 ± 0.020	0.175 ± 0.028	0.136 ± 0.017
3	0.104 ± 0.011	0.088 ± 0.006	0.110 ± 0.017	0.091 ± 0.015
5	0.100 ± 0.020	0.099 ± 0.009	0.101 ± 0.021	0.090 ± 0.012

Ni–F structures, the Ni^{2+} ion has an octahedral shell of F^- ions which is only provided at the Li^+ site in $BaLiF_3$. The charge compensation in the crystalline structure may be corrected by the existence of cationic vacancies and/or by the presence of F^- and Li^+ ions in the interstitial sites of the crystalline lattice. $BaLiF_3$ matrix itself shows intrinsic defects which are related to its minimum energy state [9]. The most likely intrinsic defect disorder involves formation of Li^+ and F^- vacancy pairs. At higher temperatures, Li^+ and F^- Frenkel pairs might be formed since their energies are also relatively low. Ion migration depends on the intrinsic disorder.

During the synthesis of the doped BLF compound, LiF is partially substituted by NiF_2 resulting in a deviation of the initial stoichiometry. As the Ni^{2+} concentration increases, the dopant will not behave anymore as an impurity but as a component of the synthesized compound. In order to study the stoichiometric variations, samples were extracted from the central part of each doped ingot, i.e. from the BLF : Ni phase, and analyzed by DTA as shown in Fig. 4. The presence of metallic nickel was not observed on the surface of the refined ingots. Curve (a) presents an endothermic peak with onset temperature of 840°C, corresponding to the melting of BLF : Ni. Additionally, a broad endothermic peak can be observed with onset temperature of 1300°C, which corresponds to the variation in the stoichiometry of the BaF_2 phase due to the Ni content. This deviation becomes more perceptible as the concentration of the dopant in the host increased, as can be observed in curves (b) and (c).

The distribution coefficient k was evaluated according to the equation [10]

$$\frac{C_s}{C_0} = \left[1 - (1-k)\exp\left(-k\frac{x}{\ell}\frac{\rho_s}{\rho_\ell}\right)\right], \tag{3}$$

where C_s is the nickel concentration at a distance x from the beginning of the solidified ingot, C_0 is the initial nickel concentration, ℓ is the liquid zone length and ρ_s and ρ_ℓ are the densities of the solid and liquid, respectively.

In order to determine the Ni^{2+} distribution coefficient in the BLF host, longitudinal samples of each refined ingot were sectioned. The samples were separated from the last solidified fraction of each selected part. Ni^{2+} content was determined using neutron activation chemical analysis. Fig. 5 shows the data fit of the Ni^{2+} distribution in the doped ingots. Two data sets were used: the first one considers the total length of the ingot (L) and the second one considers only the stoichiometric part of the ingot (L^*). The distribution coefficient k for zone-refined ingots with Ni^{2+} nominal concentrations of 3 and 5 mol% is evaluated as about 0.1 for both lengths. However, as shown in Table 2, the results for doped ingot with nominal concentration of 1 mol% have shown slightly different values. In order to check the results obtained for nickel concentration in these ingots, a second technique was used: X-ray fluorescence. The calculated k from concentration measurements by X-ray fluorescence analysis is also shown in Table 2. Similar results were obtained with 3 and 5 mol%-doped ingots in comparison with neutron activation analysis.

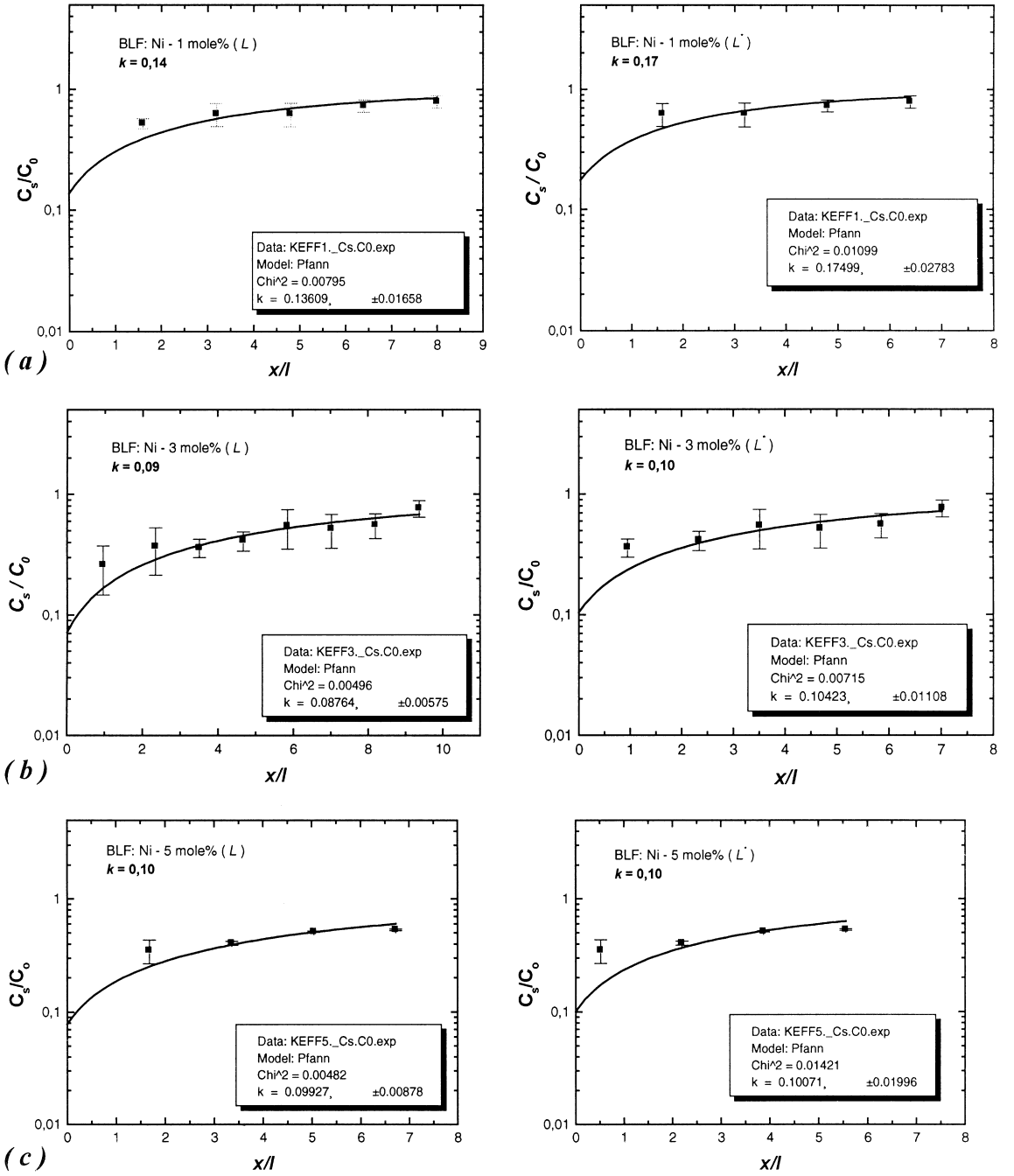

Fig. 5. Nickel distribution in the doped ingot with the nominal concentration of: (a) 1, (b) 3 and (c) 5 mol%. The total length of the ingot L (left column) and the length of the stoichiometric region L^* was considered (right column).

However, the 1 mol%-doped ingot always showed a higher distribution coefficient.

The higher value of k obtained in the lower concentration doped ingot could be attributed to an error in the neutron activation concentration measurements. In general, barium shows large neutron cross section which can interfere with the nickel measurement at low concentrations. However, a slightly different behavior in the nickel concentration along the ingots was also found using X-ray fluorescence measurements.

4. Conclusions

A zone-melting technique under reactive atmosphere was applied to the preparation of $BaLiF_3$ crystals in order to optimize the incorporation of Ni^{2+} in the matrix for optical applications.

Ni^0 formation was observed in synthesized ingots even for processes under HF flow. Thermal analysis measurements have shown that the oxidation and reduction of nickel may occur simultaneously during melting decreasing the Ni^{2+} incorporation into the crystal. These effects are more perceptible as higher is the dopant concentration in the ingots.

Zone-melting experiments were performed in synthesized ingots with 1, 3 and 5 mol% Ni^{2+}. The presence of metallic nickel was not observed on the surface of the refined ingots The distribution coefficient using neutron activation analysis was evaluated as 0.1 for the dopant concentrations of 3 and 5 mol% and as 0.15 for the lowest concentration (1 mol%). These results have shown that the low incorporation of nickel ions in BLF crystal is not only because of the oxidation and reduction reactions, but also because of the low value of the distribution coefficient of the Ni^{2+} in the BLF host.

Acknowledgements

This work was accomplished with the support from the *Fundação de Amparo à Pesquisa do Estado de Sâo Paulo*-FAPESP (Brazil).

References

[1] M. Duarte, E. Martins, S.L. Baldochi, S.P. Morato, N.D. Vieira Jr., M.M.F. Vieira, Opt. Commun. 151 (1998) 366.
[2] E. Martins, N.D. Vieira Jr., S.L. Baldochi, S.P. Morato, J.Y. Gesland, J. Lumin. 62 (1994) 281.
[3] E. Martins, M. Duarte, S.L. Baldochi, S.P. Morato, M.M.F. Vieira, N.D. Vieira Jr., J. Phys. Chem. Solid 58 (1997) 655.
[4] S.L. Baldochi, A.M.E. Santo, E. Martins, M. Duarte, M.M.F. Vieira, N.D. Vieira Jr., S.P. Morato, J. Crystal Growth 166 (1996) 375.
[5] J. Granec, L. Lozano, in: P. Hagenmuller (Ed.), Preparative Methods: Inorganic Solid Fluorides – Chemistry and Physics, Academic Press Inc., New York, 1985.
[6] A. Neuhaus, H.G. Holz, H.D. Klein, Z. Phys. Chem. Neue Folge 53 (1967) 163.
[7] A.M.E. Santo, Master in Science Thesis, IPEN-University of Sao Paulo, Brazil, 1997, p. 114.
[8] A.V. Chadwick, S.R. Davis, J.F. de Lima, M.E.G. Valério, S.L. Baldochi, J. Phys.: Condens. Matter 8 (1996) 10679.
[9] R.A. Jackson, M.E.G. Valerio, J.F. de Lima, J. Phys.: Condens. Matter 8 (1996) 10931.
[10] W.G. Pfann, Amer Inst. Mining Metall. Engrs. 194 (1952) 747.